

Enhanced negative nonlocal conductance in an interacting quantum dot connected to two ferromagnetic leads and one superconducting lead

C. Lee

*Key Laboratory of Artificial Structures and Quantum Control (Ministry of Education),
Department of Physics and Astronomy, Shanghai Jiaotong University, 800 Dongchuan Road, Shanghai 200240, China*

Bing Dong* and X. L. Lei

*Key Laboratory of Artificial Structures and Quantum Control (Ministry of Education),
Department of Physics and Astronomy, Shanghai Jiaotong University,
800 Dongchuan Road, Shanghai 200240, China and
Collaborative Innovation Center of Advanced Microstructures, Nanjing, China*

In this paper, we investigate the electronic transport properties of a quantum dot (QD) connected to two ferromagnetic leads and one superconductor lead in the Kondo regime by means of the finite- U slave boson mean field approach and nonequilibrium Green function technique. In this three-terminal hybrid nano-device, we will focus our attention on the joint effects of the Kondo correlation, superconducting proximity pairing, and spin polarization of leads. It is found that: the superconducting proximity effect will suppress the linear local conductance (LLC) stemming from the weakened Kondo peak, and when its coupling Γ_s is bigger than the tunnel-coupling Γ of two normal leads, the linear cross conductance (LCC) becomes negative in the Kondo region; for antiparallel configuration, increasing spin polarization further suppresses LLC but enhances LCC, i.e. causing larger negative values of LCC, since it is benefit for emergence of cross Andreev reflection; On the contrary, for parallel configuration, with increasing spin polarization, the LLC descends and greatly widens with the appearance of shoulders, and eventually splits into four peaks, and meanwhile the LCC reduces relatively rapidly to the normal conductance.

PACS numbers: 74.70.-b, 74.45.+c, 72.15.Qm, 73.23.Hk, 75.47.-m

I. INTRODUCTION

Recently, electron transport through hybrid nanodevice, for instance, a quantum dot (QD) connected to normal and superconducting electrodes, has attracted much attention in many experimental^{1–20} and theoretical studies,^{21–29} due to their physical challenges and potential applications in spintronics and quantum information. When a QD is connected to a superconductor, superconducting order can leak into it to give rise to pairing correlations and an induced superconducting gap, known as the superconducting proximity effect, which privileges the tunnelling of Cooper pairs of electrons with opposite spin, and thereby favours QD states with even numbers of electrons and zero total spin. At the same time, the local Coulomb repulsion enforces a one-by-one filling of the QD, and thereby induces the Coulomb blockade and even the Kondo effect at considerably low temperature, which exhibits zero-bias anomaly in the differential conductance with odd number of electrons residing in the QD. In this case, the superconducting proximity effect competes with the on-site Coulomb correlation.^{6,8,20,21,25,26,28,29}

It is even more intriguing when the QD additionally connects to a ferromagnetic lead.^{30,31} It has been already known that, the effective exchange field induced by the ferromagnetic correlation can cause spin imbalance inside the QD, and as a result, suppress and/or even split the Kondo peak in the differential conductance.^{32–36} Besides, spin polarization of the QD, on the one hand, is disadvantageous to the formation of on-dot superconducting pairing. But the spin polarization in the antiparallel con-

figuration, on the other hand, is favorable to the Andreev reflection (AR) and Cooper pair splitting.³¹ It is, therefore, very interesting to study how the interplay of the Kondo, superconducting pairing, and ferromagnetic correlations affects the electron tunneling through a QD.³⁷ In a recent paper, D. Futterer *et al* present a theoretical analysis of the subgap transport of such a three-terminal hybrid system, consist of an interacting QD attached to two ferromagnetic leads and one superconducting lead.^{38,39} They focused on the first-order sequential tunneling by using master equation and found that the strong on-dot electron-electron interaction, rather than the nonlocal AR, leads to negative values of the nonlocal current response at an appropriately large bias voltage. Moreover, the tunneling magnetoresistance has been calculated for the same system to display a nontrivial dependence on the bias voltage and the level detuning due to the AR.⁴⁰ Later on, it has been nevertheless reported that the cross AR is indeed the dominant nonlocal transport channel at low bias voltage and leads to a negative value of the cross conductance in the three terminal hybrid nanodevice with two normal electrodes instead.^{41,42}

In the present work, we extend a finite- U slave boson mean field (SBMF) approach of Kotliar and Ruckenstein⁴³ with help of the nonequilibrium Green function (NGF) method to investigate the subgap transport for the same three-terminal hybrid QD as in Ref. 38. This kind of SBF approach is generally believed to be reliable in describing not only spin fluctuations rigorously but also charge fluctuations to certain degree in the Kondo regime at zero temperature. This nonperturbative

approach has been successfully utilized to calculate the linear and nonlinear conductance within a relatively wide dot-level range from the mixed valence to the empty orbital regimes, in which the major characteristics induced by the external magnetic field and the magnetization in Kondo transport arise.^{44–47} Besides, this approach has been furthermore applied to analyze the π -phase transition in a double-QDs Josephson junction due to competition between Kondo and interdot antiferromagnetic coupling.⁴⁸ The main purpose of this paper is thereby to analyze in detail the interplay of the Kondo, superconducting proximity induced on-dot pairing, and ferromagnetic correlations and their influence on electronic tunneling.

The rest of the paper is organized as follows. In Sec.II, we introduce our model of the three-terminal hybrid system, and the equivalent slave-boson field Hamiltonian. Then we present the self-consistent equations of the expectation values of slave-boson operators within the SBMF approach and NGF method. Moreover, the formulas for current and linear conductance, including the local and cross conductances, are given. In Sec.III, we present and analyze in detail our numerical calculations for the linear conductance and nonlinear conductance. Finally, a brief summary is given in Sec.IV.

II. MODEL AND THEORETICAL FORMULATION

A. Model Hamiltonian

We consider a three-terminal hybrid nanodevice: an interaction QD connected to one superconducting lead and two ferromagnetic leads, as shown in Fig. 1. The Hamiltonian of the system can be written as:³⁸

$$H = H_L + H_R + H_{QD} + H_T, \quad (1)$$

where

$$H_\eta = \sum_{k\sigma} \epsilon_{\eta k\sigma} c_{\eta k\sigma}^\dagger c_{\eta k\sigma}, \quad (2)$$

$$H_{QD} = \sum_{\sigma} \epsilon_d c_{d\sigma}^\dagger c_{d\sigma} + U n_1 n_2 + \Gamma_s (c_{d1}^\dagger c_{d2}^\dagger + c_{d1} c_{d2}), \quad (3)$$

$$H_T = \sum_{\eta k\sigma} \left(V_{\eta k} c_{\eta k\sigma}^\dagger c_{d\sigma} + \text{H.c.} \right). \quad (4)$$

Here $\eta = L, R$ denotes the left and right leads, while $\sigma = 1, 2$ represents the spin degree of freedom. In the above equations, $c_{\eta k\sigma}^\dagger$ ($c_{\eta k\sigma}$) and $c_{d\sigma}^\dagger$ ($c_{d\sigma}$) are creation (annihilation) operators of electrons with spin σ in the η th ferromagnetic lead and in the QD respectively. In the dot Hamiltonian H_{QD} , ϵ_d is the energy level of the QD,

$n_\sigma = c_{d\sigma}^\dagger c_{d\sigma}$, and U is the on-site Coulomb repulsion between opposite spin electrons. H_T depicts the tunneling between the QD and the two ferromagnetic leads, and $V_{\eta k}$ is the corresponding tunneling matrix element. In general, the tunneling amplitude $V_{\eta k}$ is assumed to be independent of spin and energy, and thus the effect of spin-polarized tunneling is captured by the spin-dependent tunneling rates, $\Gamma_{\eta\sigma} = 2\pi \sum_k |V_{\eta k}|^2 \delta(\omega - \epsilon_{\eta k\sigma})$.

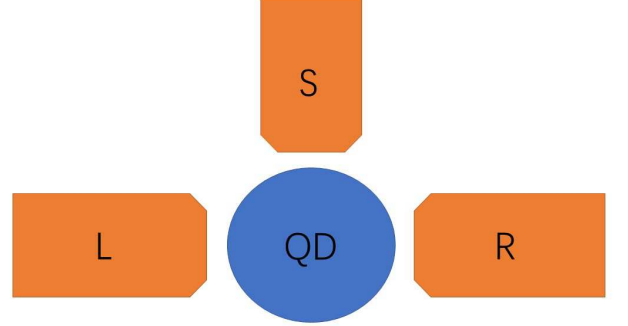


Fig. 1: (Colour online) Schematic diagram of a quantum dot connected to one superconducting lead and two ferromagnetic leads.

In this paper, since we are only interested in the subgap tunneling, it is natural to consider the limit of extremely large superconducting gap in the superconducting lead. Therefore, the degree of freedom of the superconducting lead can be integrated out and an effective term can be constructed in the dot Hamiltonian, the third term in Eq. (3). The parameter Γ_s plays indeed the role of describing the superconducting proximity effect on the dot. It is evident that this new proximized term mixes the empty state $|0\rangle$ and the doubly occupied state $|\uparrow\downarrow\rangle$ in the dot, and results in two new eigenstates with energies, $E_{\pm} = \epsilon \pm \sqrt{\epsilon^2 + 4\Gamma_s^2}$ (here $\epsilon = \epsilon_d + U/2$), which are known as the Andreev bound states. What we are interested in this paper is the effect of Andreev reflection on the electron tunneling through an interacting QD in the Kondo regime.

According to the finite- U slave-boson approach, one can introduce additional four auxiliary boson operators e , p_σ , and d , which are associated respectively with the empty, singly occupied, and doubly occupied electron states of the QD, to discuss the above problem without interparticle couplings in an enlarged space with constraints: the completeness relation,⁴³

$$\sum_{\sigma} p_\sigma^\dagger p_\sigma + e^\dagger e + d^\dagger d = 1, \quad (5)$$

and the particle number conservation condition,

$$c_{d\sigma}^\dagger c_{d\sigma} = p_\sigma^\dagger p_\sigma + d^\dagger d. \quad (6)$$

Within the mean-field scheme, the effective Hamiltonian becomes:⁴³

$$\begin{aligned}
H = & \sum_{\sigma} \epsilon_d c_{d\sigma}^{\dagger} c_{d\sigma} + U d^{\dagger} d + \Gamma_s (z_1^* z_2^* c_{d1}^{\dagger} c_{d2}^{\dagger} + z_1 z_2 c_{d1} c_{d2}) + \sum_{\eta k \sigma} (V_{\eta k} c_{\eta k \sigma}^{\dagger} c_{d\sigma} z_{\sigma} + V_{\eta k}^* c_{d\sigma}^{\dagger} c_{\eta k \sigma} z_{\sigma}^*) \\
& + \sum_{\eta k \sigma} \epsilon_{\eta k \sigma} c_{\eta k \sigma}^{\dagger} c_{\eta k \sigma} + \lambda^1 (\sum_{\sigma} p_{\sigma}^{\dagger} p_{\sigma} + e^{\dagger} e + d^{\dagger} d - 1) + \sum_{\sigma} \lambda_{\sigma}^2 (c_{d\sigma}^{\dagger} c_{d\sigma} - p_{\sigma}^{\dagger} p_{\sigma} - d^{\dagger} d),
\end{aligned} \tag{7}$$

where three Lagrange multipliers λ^1 and λ_{σ}^2 are drawn in order to make the constraints valid, and z_{σ} is the correctional parameters in the hopping term to recover the many-body effect on tunneling with

$$z_{\sigma} = (1 - d^{\dagger} d - p_{\sigma}^{\dagger} p_{\sigma})^{-1/2} (e^{\dagger} p_{\sigma} + p_{\sigma}^{\dagger} d) (1 - e^{\dagger} e - p_{\sigma}^{\dagger} p_{\sigma})^{-1/2}. \tag{8}$$

B. Self-consistent equations

From the effective Hamiltonian Eq. (7), one can derive four equations of motion of slave-boson operators, which serve as the basic equations together with the three constraints. Then we apply further the mean-field approximation in the statistical expectations of these equations, where all the boson operators are replaced by their respective expectation values. After a lengthy and tedious calculation by employing Langreth technique, we can obtain the self-consistent equations as follows:⁴⁴⁻⁴⁷

$$\Gamma_s \frac{\partial(z_1 z_2)}{\partial e} (R + R^*) + 2\lambda^1 e + \sum_{\sigma} p_{\sigma} (Q_{\sigma} + Q_{\sigma}^*) = 0, \tag{9}$$

$$\Gamma_s \frac{\partial(z_1 z_2)}{\partial p_1} (R + R^*) + 2(\lambda^1 - \lambda_1^2) p_1 + e(Q_1 + Q_1^*) + d(Q_2 + Q_2^*) = 0, \tag{10}$$

$$\Gamma_s \frac{\partial(z_1 z_2)}{\partial p_2} (R + R^*) + 2(\lambda^1 p_2 - \lambda_2^2) p_2 + d(Q_1 + Q_1^*) + e(Q_2 + Q_2^*) = 0, \tag{11}$$

$$\Gamma_s \frac{\partial(z_1 z_2)}{\partial d} (R + R^*) + 2(U + \lambda^1 d - \sum_{\sigma} \lambda_{\sigma}^2) d + \sum_{\sigma} p_{\sigma} (Q_{\sigma} + Q_{\sigma}^*) = 0, \tag{12}$$

$$\sum_{\sigma} |p_{\sigma}|^2 + |e|^2 + |d|^2 - 1 = 0, \tag{13}$$

$$K_{\sigma} - |p_{\sigma}|^2 - |d|^2 = 0, \tag{14}$$

where

$$K_1 = \frac{1}{2\pi i} \int d\omega G_{d11}^<(\omega), \tag{15}$$

$$K_2 = \frac{-1}{2\pi i} \int d\omega G_{d22}^<(\omega), \tag{16}$$

$$R = \frac{1}{2\pi i} \int d\omega G_{d21}^<(\omega), \tag{17}$$

$$\begin{aligned}
Q_{1\eta} = & z_1 \Gamma_{\eta 1} \int \frac{d\omega}{2\pi} \left\{ -\frac{i}{2} \left[\tilde{\Gamma}_{L1} f_L(\omega) + \tilde{\Gamma}_{R1} f_R(\omega) \right] |G_{d11}^R(\omega)|^2 \right. \\
& \left. - \frac{i}{2} \left[\tilde{\Gamma}_{L2} (1 - f_L(-\omega)) + \tilde{\Gamma}_{R1} (1 - f_R(-\omega)) \right] |G_{d21}^R(\omega)|^2 + f_{\eta}(\omega) G_{d11}^A(\omega) \right\},
\end{aligned} \tag{18}$$

$$Q_{2\eta} = z_2 \Gamma_{\eta 2} \int \frac{d\omega}{2\pi} \left\{ \frac{i}{2} \left[\tilde{\Gamma}_{L1}(1 - f_L(\omega)) + \tilde{\Gamma}_{R1}(1 - f_R(\omega)) \right] |G_{d21}^R(\omega)|^2 \right. \\ \left. + \frac{i}{2} \left[\tilde{\Gamma}_{L2} f_L(-\omega) + \tilde{\Gamma}_{R1} f_R(-\omega) \right] |G_{d22}^R(\omega)|^2 - f_\eta(-\omega) G_{d22}^A(\omega) \right\}, \quad (19)$$

and

$$Q_\sigma = \sum_\eta Q_{\sigma\eta}. \quad (20)$$

Here the QD Keldysh NGFs, $G_{d\sigma\sigma'}^{R(A,<)}(\omega)$ are the matrix elements of the 2×2 retarded (advanced and correlation) GF matrix $G_d^{R(A,<)}(\omega) = \langle\langle \phi; \phi^\dagger \rangle\rangle^{R(A,<)}$ defined in the Nambu presentation, in which the mixture Fermion operator, $\phi = (c_{d1}, c_{d2}^\dagger)^T$, has to be introduced to describe electronic dynamics due to the superconducting proximity effect. For the effective noninteracting Hamiltonian, the retarded and advanced GFs $G_d^{R(A)}$ can be easily written in the frequency domain as:

$$\left(G^{R(A)}(\omega) \right)^{-1} = \begin{bmatrix} \omega - \epsilon_d - \lambda_1^2 \pm \frac{i}{2}(\tilde{\Gamma}_{L1} + \tilde{\Gamma}_{R1}) & -\Gamma_s z_1 z_2 \\ -\Gamma_s z_1^* z_2^* & \omega + \epsilon_d + \lambda_2^2 \pm \frac{i}{2}(\tilde{\Gamma}_{L2} + \tilde{\Gamma}_{R2}) \end{bmatrix}. \quad (21)$$

with the renormalized parameters, $\tilde{\Gamma}_{\eta\sigma} = |z_\sigma|^2 \Gamma_{\eta\sigma}$. And the correlation GF $G_d^<(\omega)$ can be obtained with the help of the following Keldysh relation typical for a noninteracting system,

$$G_d^<(\omega) = G_d^R(\omega) \Sigma_\phi^<(\omega) G_d^A(\omega), \quad (22)$$

with the self-energy,

$$\Sigma_\phi^<(\omega) = \sum_\eta 2\pi i \begin{bmatrix} \tilde{\Gamma}_{\eta 1} f_\eta(\omega) & 0 \\ 0 & \tilde{\Gamma}_{\eta 2} [1 - f_\eta(-\omega)] \end{bmatrix}, \quad (23)$$

where $f_\eta(\omega) = 1/(e^{\beta(\omega - \mu_\eta)} + 1)$ is the Fermi distribution function of the lead η with the chemical potential μ_η and temperature $1/\beta$.

C. The current and linear conductance

The electric current flowing from the lead η into the QD can be obtained from the rate of change of electron number operator of the left lead,

$$I_\eta = \sum_\sigma I_{\eta\sigma} = -e \sum_\sigma \left\langle \frac{d}{dt} \sum_k c_{\eta k\sigma}^\dagger c_{\eta k\sigma} \right\rangle. \quad (24)$$

After standard calculation, the current for the left lead can be written as^{41,42}

$$I_L = I_L^{ET} + I_L^{DAR} + I_L^{CAR}, \quad (25)$$

with

$$I_L^{ET} = \frac{e}{h} \int d\omega \left\{ \tilde{\Gamma}_{L1} \tilde{\Gamma}_{R1} [f_L(\omega) - f_R(\omega)] |G_{d11}^R(\omega)|^2 \right. \\ \left. + \tilde{\Gamma}_{L2} \tilde{\Gamma}_{R2} [f_L(-\omega) - f_R(-\omega)] |G_{d22}^R(\omega)|^2 \right\}, \quad (26)$$

$$I_L^{DAR} = \frac{2e}{h} \int d\omega \tilde{\Gamma}_{L1} \tilde{\Gamma}_{L2} [f_L(\omega) + f_L(-\omega) - 1] \\ \times |G_{d12}^R(\omega)|^2, \quad (27)$$

$$I_L^{CAR} = \frac{e}{h} \int d\omega \left\{ \tilde{\Gamma}_{L1} \tilde{\Gamma}_{R2} [f_L(\omega) + f_R(-\omega) - 1] \right. \\ \left. + \tilde{\Gamma}_{L2} \tilde{\Gamma}_{R1} [f_L(-\omega) + f_R(\omega) - 1] \right\} |G_{d12}^R(\omega)|^2. \quad (28)$$

The corresponding currents for the right lead can be readily obtained by simply exchanging the subscripts L and R in Eqs. (26)-(28). It is found that the current can be divided into three parts: I_L^{ET} describes the single-particle tunneling current due to the normal electron transfer (ET) processes from the left lead directly to the right lead; I_L^{DAR} denotes the local Andreev current due to the direct AR (DAR) processes in which an electron injecting from the left lead forms a Cooper pair in the superconducting lead and, at the same time, is reflected as a hole back into the left lead; while I_L^{CAR} is the nonlocal Andreev current due to the crossed AR (CAR) processes which is similar to DAR except that hole is reflected into another lead, i.e., here the right lead.

Since we are interested in the interplay between the Andreev bound state and the Kondo effect in the nonlocal subgap tunneling, we choose the bias voltage configuration in this hybrid three-terminal nanodevice as follows: the left lead is biased with the chemical potential V , while the right lead and the superconducting electrode are both in contact with ground. Therefore, one can define two different linear conductances, the usual local conductance $G_L = \partial I_L / \partial V|_{V=0}$ and the unusual nonlocal (cross) conductance $G_C = \partial I_R / \partial V|_{V=0}$, which is related to the nonlocal current response of the hybrid three-terminal nanodevice to external driving field, i.e., current flowing in the right lead due to the bias voltage applied to the left lead. From Eqs. (26)-(28), the local

conductance reads

$$G_L = \left. \frac{\partial I_L}{\partial V} \right|_{V=0} = G^{ET} + G^{DAR} + G^{CAR}, \quad (29)$$

and the cross conductance is

$$G_C = \left. \frac{\partial I_R}{\partial V} \right|_{V=0} = G^{ET} - G^{CAR}, \quad (30)$$

where

$$G^{ET} = \frac{e^2}{h} \left(\tilde{\Gamma}_{L1} \tilde{\Gamma}_{R1} |G_{d11}^R(0)|^2 + \tilde{\Gamma}_{L2} \tilde{\Gamma}_{R2} |G_{d22}^R(0)|^2 \right), \quad (31)$$

$$G^{DAR} = \frac{4e^2}{h} \tilde{\Gamma}_{L1} \tilde{\Gamma}_{L2} |G_{d12}^R(0)|^2, \quad (32)$$

$$G^{CAR} = \frac{e^2}{h} \left(\tilde{\Gamma}_{L1} \tilde{\Gamma}_{R2} + \tilde{\Gamma}_{R1} \tilde{\Gamma}_{L2} \right) |G_{d12}^R(0)|^2. \quad (33)$$

It is obvious that all of the three different tunneling processes have contribution to the local conductance. Nevertheless the DAR tunneling process, as expected, has no contribution to the cross conductance. More interestingly, the CAR tunneling process provides a contrary contribution, in comparison with the ET process, to the cross conductance Eq. (30), which is responsible for the negative value of the cross conductance in certain appropriate conditions as shown in the following section. This opposite role of the CAR can be interpreted in an intuitive way: a hole entering the right lead is physically equivalent to an electron injuring into the QD from the right lead, thus resulting in an opposite current flowing in the right lead. It is important to point out that if the superconducting coupling is switched off ($\Gamma_s = 0$), there are no DAR and CAR processes and as a result, the cross conductance reduces to the local conductance.

III. RESULT AND DISCUSSION

We suppose that the left and right leads are made from the identical material and in the wide band limit, of interest in the present investigation, the ferromagnetism of the leads can be accounted for by the polarization-dependent couplings $\Gamma_{L1} = \Gamma_{R1} = (1+p)\Gamma$, $\Gamma_{L2} = \Gamma_{R2} = (1-p)\Gamma$ for the parallel (P) alignment, while $\Gamma_{L1} = \Gamma_{R2} = (1+p)\Gamma$, $\Gamma_{L2} = \Gamma_{R1} = (1-p)\Gamma$ for the anti-parallel (AP) alignment. Here Γ describes the tunneling coupling between the QD and the nonmagnetic leads, which is taken as the energy unit in the following calculations. And p ($0 \leq p < 1$) denotes the polarization strength of the leads.

In the following we will deal with the three-terminal QD system having a fixed finite Coulomb interaction $U = 10$ at zero temperature and consider effects of changing bare dot level ϵ_d and the spin polarization p , and proximity strength Γ_s respectively.

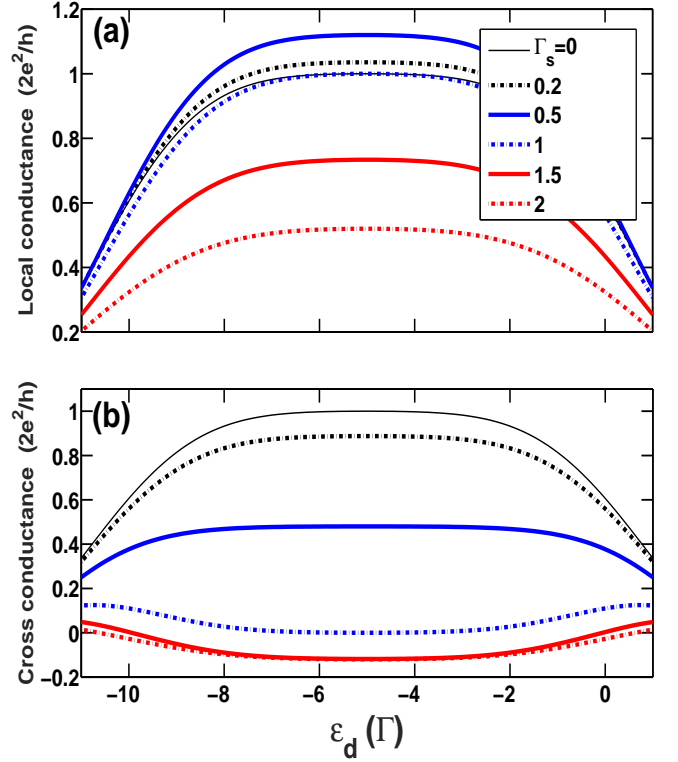


Fig. 2: (Colour online) (a) The local conductance and (b) the cross conductance versus the bare dot level ϵ_d for different proximity-coupling strengths Γ_s in the case of normal leads, i.e., $p = 0$.

A. Linear local and cross conductances

We show, at first, the calculated linear conductances in Fig. 2, including the local conductance G_L and the non-local cross conductance G_C as functions of the bare energy level ϵ_d of the QD at different superconducting coupling strengths $\Gamma_s = 0, 0.2, 0.5, 1.0, 1.5$, and 2.0 in the case of no spin-polarization $p = 0$. Without the superconducting coupling $\Gamma_s = 0$, $G_L = G_C$ and the linear conductance reaches the unitary limit, G_0 ($G_0 \equiv 2e^2/h$), as expected in the Kondo regime. With increasing the coupling Γ_s , the local conductance G_L raises at the beginning, as seen in Fig. 2(a), since the AR channel starts to emerge and make contribution to the electronic tunneling. A little bit bigger value of the conductance, $G_L \simeq 1.1G_0$, than the unitary limit of conductance of single-particle tunneling is reached at the coupling $\Gamma_s = 0.5$ in the Kondo regime. It is important to notice that such bigger value of the conductance is a signature indicating that the tunneling event in the present hybrid system is mixture of the single-particle and Cooper pair tunnelings. Increasing further the coupling Γ_s will, however, cause decrease of the local conductance G_L . The suppression of G_L can be interpreted as follows: electron coming from the left lead has much more higher probability to form the Cooper pair injuring into the superconducting electrode due to the considerably strong coupling $\Gamma_s > 0.5\Gamma$, and as a result, the ET process is rapidly suppressed. Different

from the local conductance, the nonlocal conductance G_C decreases from the beginning and even becomes negative if the proximity-coupling is sufficiently strong. The negative cross conductance means that, when the left lead is applied voltage bigger than the right lead, electrons will, instead of entering into the right lead from the QD, tunnel into the QD out of the right lead. Moreover, we find that when the QD leaves the Kondo regime, the cross conductance will become positive again.

Such effects of Γ_s are clearly manifested in Fig. 3, in which the local and nonlocal conductances, and their three respective parts, G^{ET} , G^{DAR} , and G^{CAR} as well, are illustrated as functions of the coupling Γ_s for the specific system having bare dot level, $\epsilon_d = -U/2 = -5$. It is observed that: a maximum value of the local conductance, $G_L = 1.125G_0$ is arrived at $\Gamma_s = 0.58\Gamma$; After that point of Γ_s , the AR process becomes the predominate tunneling mechanism over the ET process; When the proximity-coupling is equal to the tunnel-coupling, i.e. $\Gamma_s = \Gamma$, a new resonance is reached originated from interplay between the Kondo effect and AR. As consequences, $G^{DAR} = G_0/2$ and $G^{CAR} = G^{ET} = G_0/4$, and the local conductance is thus arrived at the unitary value, $G_L = G_0$ again. At the same time, the nonlocal conductance is completely vanished, $G_C = 0$, which indicates no current response in the right lead to the bias voltage applied to the left lead.

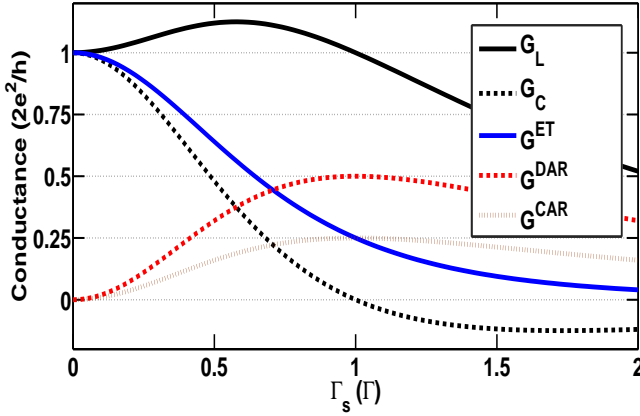


Fig. 3: (Colour online) The local conductance (black-solid line) and the cross conductance (black-dotted line) versus the proximity coupling Γ_s for the system with a bare dot level at the particle-hole symmetric point, $\epsilon_d = -U/2 = -5$ in the case of normal leads. The three parts of the conductance are also plotted as well for illustration.

Secondly, we investigate the cross conductance G_C as a function of the bare energy level ϵ_d of the QD at different proximity couplings Γ_s in the AP configuration with a large spin polarization $p = 0.5$ in Fig. 4. In the AP configuration, similar with the case of zero spin polarization $p = 0$, electrons with up-spin and down-spin are equally available in the whole system, favoring the formation of the Kondo-correlated state within a wide dot level range centered at $\epsilon_d = -U/2 = -5$. Meanwhile, since there is no splitting of the renormalized dot levels, $\epsilon_d + \lambda_\sigma^2$, for

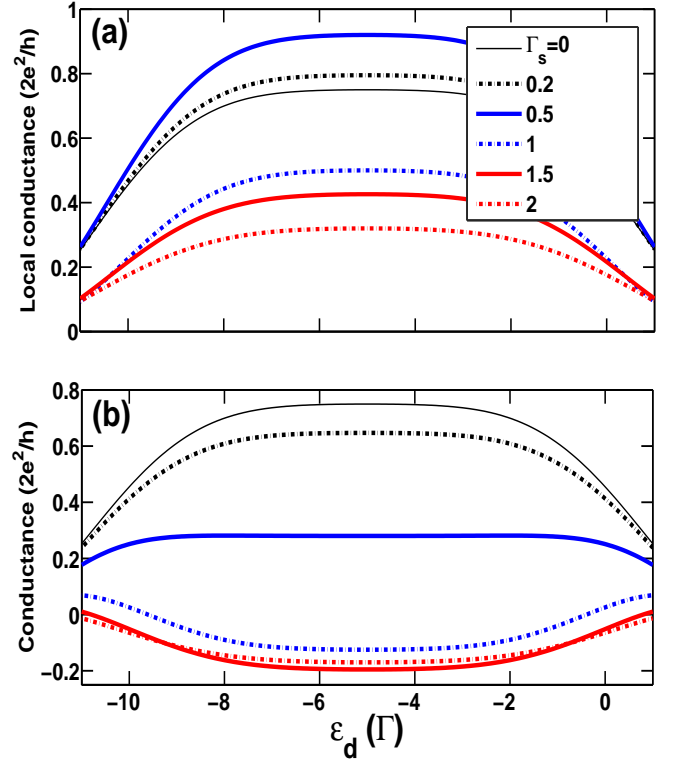


Fig. 4: (Colour online) (a) The local conductance and (b) the cross conductance versus the bare dot level ϵ_d for different proximity-coupling strengths Γ_s in the AP configuration with $p = 0.5$.

different spins, the usual tunneling and charging peaks, around $\epsilon_d = 0$ and $-U$ respectively, are relatively narrow. The local conductance G_L -vs.- ϵ_d curves show similar behavior with the case of zero spin polarization even in the presence of superconducting coupling Γ_s . Furthermore, since no spin-flip scattering exists in the tunneling processes, in the AP configuration the majority-spin (e.g. up-spin) states in the left lead increase but the available up-spin (minority-spin) states in the right lead decrease with increasing spin polarization strength, and as a consequence the transfer of the majority-spin (up-spin) electrons through the QD is suppressed, such that the local conductance goes down and eventually vanishes at $p = 1$ as expected. On the contrary, the available down-spin states in the right lead indeed increase in the AP configuration, which just facilitates occurrence of the CAR process.³¹ Therefore, one can observe that G_C becomes negative at almost the whole region of dot levels, from the mixed-valence regime to the empty orbital regime even when $\Gamma_s < 1$, and arrives nearly at a considerably bigger negative value, $G_C \simeq -G_0/5$, at the Kondo regime at $p = 0.5$. It is physically interesting to consider the extreme case of $p = 1$. As mentioned above, in the AP configuration electrons with up-spin and down-spin are identical with each other, preferring the formation of the Kondo-correlated state for all values of p . However, since the up-spin states are almost unavailable in the right lead in the case of large polar-

ization, the ET process for the left lead to the right lead is completely damaged (implying an exactly vanishing conductance in the usual QD system), but the CAR process survives here as unique tunneling mechanism and makes contribution to electronic tunneling exclusively. It is anticipated that in this case, $G^{ET} = G^{DAR} = 0$ and $G_L = -G_C = G^{CAR} = G_0/2$ (this is the unitary limit of conductance of single channel).

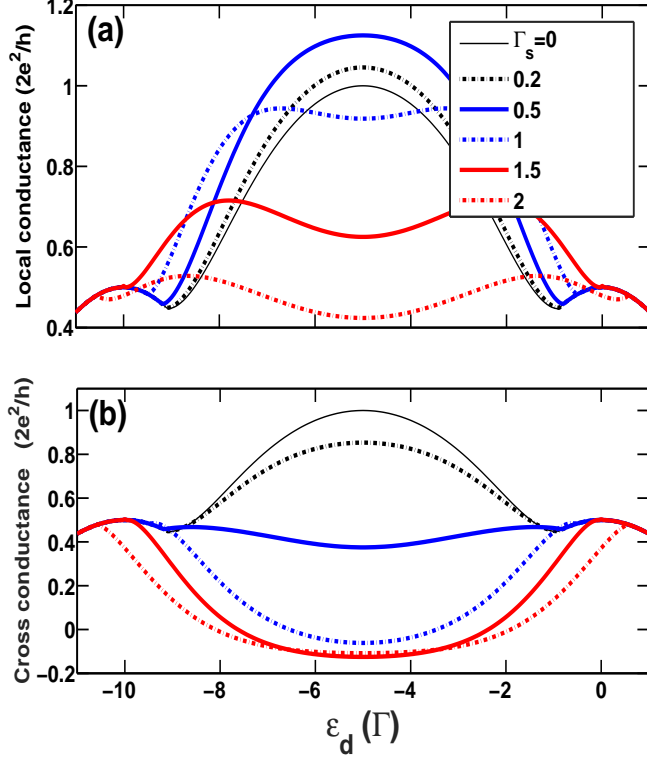


Fig. 5: (Colour online) (a) The local conductance and (b) the cross conductance versus the bare dot level ϵ_d for different proximity-coupling strengths Γ_s in the P configuration with $p = 0.5$.

The situation is quite different in the case of P configuration, as demonstrated in Fig. 5, in which the two conductances are plotted as functions of bare dot level with spin polarization $p = 0.5$. In the P configuration, finite spin polarization splits the dot level for up and down spins and thus broadens the usual resonance peaks around $\epsilon_d = 0$ and $\epsilon_d = -U$.^{32–36} On one hand, since minority-spin electrons are still available in the two electrodes to build Kondo screening correlation to certain degree, the central Kondo peak can still be reached at the unitary limit G_0 at the large polarization $p = 0.5$ in the case of $\Gamma_s = 0$. On the other hand, the number of minority-spin electrons is too small to construct the Kondo-correlated state at $p = 0.5$ and thus Kondo-induced conductance enhancement disappears rapidly when the QD leaves away from the particle-hole symmetric point $\epsilon_d = -U/2$. These two factors cause the appearance of kinks or splitting peaks in the both conductance- ϵ_d curves. Besides, it is observed from Fig. 5(a) that the central Kondo peak in the local conductance is also

progressively splitting with increasing proximity coupling $\Gamma_s \geq \Gamma$ in this P configuration. Furthermore, decrease of minority-spin states in both leads in the P configuration hinders emergence of AR processes, which leads to weakly negative cross conductance in the Kondo regime, e.g. $G_C \geq -0.1G_0$, and even totally vanished CAR, thus $G_C \simeq G_L$, at the two usual resonance peaks as shown in Fig. 5(b). It states that strong ferromagnetism destroys proximitized superconductivity in this three-terminal hybrid nanosystem.

B. Nonlinear local and cross Conductances

Now we turn to investigation of nonlinear tunneling, since the nonlinear differential conductance dI_L/dV is believed to be a very useful tool in experiments to detect the formation of the Kondo-correlated state due to its proportionality to transmission spectrum, supposed that the total transmission is unchanged subject to external bias voltage. In the present three-terminal hybrid device, one can define the local and cross differential conductances, $g_L = \partial I_L/\partial V$ and $g_C = \partial I_R/\partial V$, if the bias voltage V is applied to the left lead and meanwhile the superconductor and the right lead are kept grounded. From the current formulas Eqs. (25)–(28), we can then obtain that the two differential conductances are both proportional to the normal transmission spectrum $T_N(\omega)$ and the AR spectrum $T_A(\omega)$ at $\omega = V$ at zero temperature, $g_L \propto T_N(V) + aT_A(V)$ and $g_C \propto T_N(V) - bT_A(V)$ (a and b are constants).

Figure 6 shows the local and cross differential conductances as functions of bias voltage at various proximity couplings Γ_s for the system having a single dot level $\epsilon_d = -5$ at the Kondo regime. These curves for weak proximity coupling $\Gamma_s < \Gamma$ present a single zero-bias anomaly, being the signature of the Kondo effect. Nevertheless, there appears nonzero-bias peak with increasing proximity coupling $\Gamma_s \geq \Gamma$. It is announced that the Kondo correlation enhances not only the normal ET but also the AR, nonetheless the increasing superconducting proximity coupling induces splitting of the Kondo peaks in the normal transmission spectrum and the AR spectrum as well. This peak splitting is the reason that three parts of the linear conductance are all suppressed when $\Gamma_s > \Gamma$ as shown in Fig. 3. Finally, one can observe that the negative cross differential conductance becomes positive at the case of large bias voltage. External bias voltage plays a role of dissipation so as to destroy not only the Kondo correlation but the negative nonlocal current response as well.

IV. CONCLUSION

We have theoretically investigated the subgap transport properties of a hybrid nanosystem consisting of an interacting QD connected to one superconducting lead and two ferromagnetic leads. Based on finite- U slave

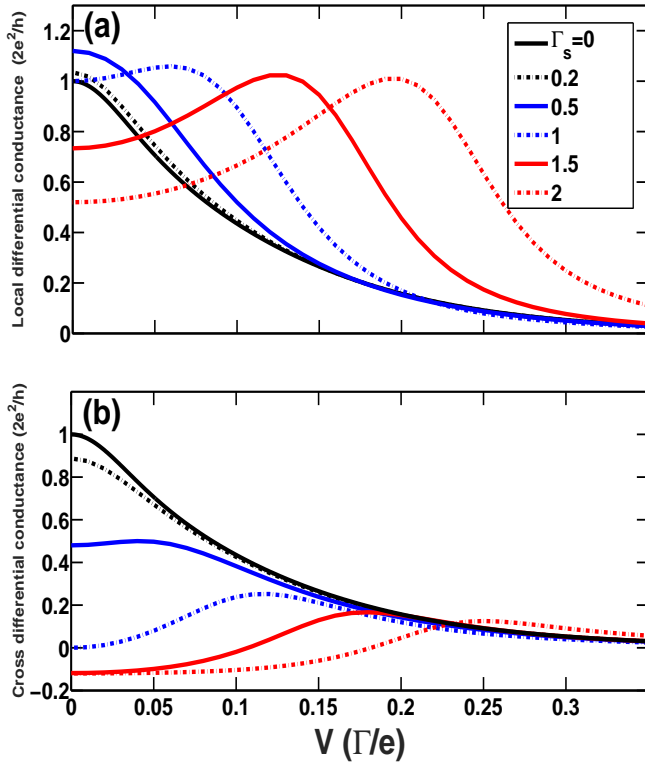


Fig. 6: (Colour online) The zero-temperature local (a) and cross (b) differential conductances versus bias voltage V for various couplings Γ_s for the system with bare dot level $\epsilon_d = -5$ in the case of normal leads ($p = 0$).

boson mean field approach and NGF method, we find markedly rich transport features ascribed to the competition among the Kondo correlation, superconducting proximity effect, and spin polarization of electrodes. In the case of weak superconducting proximity coupling, the Kondo-correlated state can still be built leading to a single zero-bias peak in the voltage-dependent differential conductance. But the peak height drops down gradually with increasing Γ_s , and when $\Gamma_s \geq \Gamma$, a non-zero peak appears. Such strong proximity coupling induces linear cross conductance negative in the Kondo region. Spin polarization can further enhance opposite current response in the right lead, i.e. more negative cross conductance, in the AP configuration, because such configuration is advantageous to the emergence of CAR. In contrast, in the P configuration, rising spin polarization p blocks CAR process and also splits the Kondo peak, such that the linear local conductance exhibits four peaks behavior when $\Gamma_s \geq \Gamma$, and the linear cross conductance reduces to the normal positive conductance more rapidly.

Acknowledgments

This work was supported by Projects of the National Science Foundation of China under Grant No. 11674223.

* Author to whom correspondence should be addressed. Email: bdong@sjtu.edu.cn.

¹ S. Russo, M. Kroug, T. M. Klapwijk, and A. F. Morpurgo, Phys. Rev. Lett. **95**, 027002 (2005), URL <https://link.aps.org/doi/10.1103/PhysRevLett.95.027002>.

² P. Cadden-Zimansky and V. Chandrasekhar, Phys. Rev. Lett. **97**, 237003 (2006), URL <https://link.aps.org/doi/10.1103/PhysRevLett.97.237003>.

³ P. Jarillo-Herrero, J. A. Van Dam, and L. P. Kouwenhoven, Nature **439**, 953 (2006).

⁴ J. A. Van Dam, Y. V. Nazarov, E. P. Bakkers, S. De Franceschi, and L. P. Kouwenhoven, Nature **442**, 667 (2006).

⁵ K. Grove-Rasmussen, H. I. Jørgensen, B. M. Andersen, J. Paaske, T. S. Jespersen, J. Nygård, K. Flensberg, and P. E. Lindelof, Phys. Rev. B **79**, 134518 (2009), URL <https://link.aps.org/doi/10.1103/PhysRevB.79.134518>.

⁶ M. R. Buitelaar, T. Nussbaumer, and C. Schönenberger, Phys. Rev. Lett. **89**, 256801 (2002), URL <https://link.aps.org/doi/10.1103/PhysRevLett.89.256801>.

⁷ S. D. Franceschi, L. Kouwenhoven, C. Schönenberger, and W. Wernsdorfer, Nature Nanotechnology **5**, 703 (2010).

⁸ K. J. Franke, G. Schulze, and J. I. Pascual, Science **332**, 940 (2011), ISSN 0036-8075, <https://science.sciencemag.org/content/332/6032/940.full.pdf>, URL <https://science.sciencemag.org/content/332/6032/940>.

⁹ T. Dirks, T. L. Hughes, S. Lal, B. Uchoa, Y.-F. Chen, C. Chialvo, P. M. Goldbart, and N. Mason, Nature Physics **7**, 386 (2011).

¹⁰ J. Schindele, A. Baumgartner, and C. Schönenberger, Phys. Rev. Lett. **109**, 157002 (2012), URL <https://link.aps.org/doi/10.1103/PhysRevLett.109.157002>.

¹¹ B. Braunecker, P. Burset, and A. Levy Yeyati, Phys. Rev. Lett. **111**, 136806 (2013), URL <https://link.aps.org/doi/10.1103/PhysRevLett.111.136806>.

¹² E. J. H. Lee, X. Jiang, M. Houzet, R. Aguado, C. M. Lieber, and S. D. Franceschi, Nature Nanotechnology **9**, 79 (2014).

¹³ R. S. Deacon, A. Oiwa, J. Sailer, S. Baba, Y. Kanai, K. Shibata, K. Hirakawa, and S. Tarucha, Nature Communications **6**, 7446 (2015).

¹⁴ G. Fülöp, F. Domínguez, S. d'Hollosy, A. Baumgartner, P. Makk, M. H. Madsen, V. A. Guzenko, J. Nygård, C. Schönenberger, A. Levy Yeyati, et al., Phys. Rev. Lett. **115**, 227003 (2015), URL <https://link.aps.org/doi/10.1103/PhysRevLett.115.227003>.

¹⁵ S. M. Albrecht, A. P. Higginbotham, M. Madsen, F. Kuemmeth, T. S. Jespersen, J. Nygård, P. Krogstrup, and C. M. Marcus, Nature **531**, 206 (2016).

¹⁶ L. Hofstetter, S. Csonka, J. Nygård, and C. Schönenberger, Nature **461**, 960 (2009).

¹⁷ R. M. Lutchyn, J. D. Sau, and S. Das Sarma, Phys. Rev. Lett. **105**, 077001 (2010), URL <https://link.aps.org/doi/10.1103/PhysRevLett.105.077001>.

¹⁸ M. Ruby, F. Pientka, Y. Peng, F. von Oppen, B. W. Heinrich, and K. J. Franke,

- Phys. Rev. Lett. **115**, 087001 (2015), URL <https://link.aps.org/doi/10.1103/PhysRevLett.115.087001>.
- ¹⁹ M. Ruby, Y. Peng, F. von Oppen, B. W. Heinrich, and K. J. Franke, Phys. Rev. Lett. **117**, 186801 (2016), URL <https://link.aps.org/doi/10.1103/PhysRevLett.117.186801>.
 - ²⁰ T. Sand-Jespersen, J. Paaske, B. M. Andersen, K. Grove-Rasmussen, H. I. Jørgensen, M. Aagesen, C. B. Sørensen, P. E. Lindelof, K. Flensberg, and J. Nygård, Phys. Rev. Lett. **99**, 126603 (2007), URL <https://link.aps.org/doi/10.1103/PhysRevLett.99.126603>.
 - ²¹ J. C. Cuevas, A. Levy Yeyati, and A. Martín-Rodero, Phys. Rev. B **63**, 094515 (2001), URL <https://link.aps.org/doi/10.1103/PhysRevB.63.094515>.
 - ²² J. Eldridge, M. G. Pala, M. Governale, and J. König, Phys. Rev. B **82**, 184507 (2010), URL <https://link.aps.org/doi/10.1103/PhysRevB.82.184507>.
 - ²³ D. S. Golubev and A. D. Zaikin, Phys. Rev. B **82**, 134508 (2010), URL <https://link.aps.org/doi/10.1103/PhysRevB.82.134508>.
 - ²⁴ A. G. Moghaddam, M. Governale, and J. König, Phys. Rev. B **85**, 094518 (2012), URL <https://link.aps.org/doi/10.1103/PhysRevB.85.094518>.
 - ²⁵ G. Kiršanskas, M. Goldstein, K. Flensberg, L. I. Glazman, and J. Paaske, Phys. Rev. B **92**, 235422 (2015), URL <https://link.aps.org/doi/10.1103/PhysRevB.92.235422>.
 - ²⁶ Y. Yamada, Y. Tanaka, and N. Kawakami, Phys. Rev. B **84**, 075484 (2011), URL <https://link.aps.org/doi/10.1103/PhysRevB.84.075484>.
 - ²⁷ A. Koga, Phys. Rev. B **87**, 115409 (2013), URL <https://link.aps.org/doi/10.1103/PhysRevB.87.115409>.
 - ²⁸ R. Žitko, Phys. Rev. B **93**, 195125 (2016), URL <https://link.aps.org/doi/10.1103/PhysRevB.93.195125>.
 - ²⁹ A. Martín-Rodero and A. L. Yeyati, Advances in Physics **60**, 899 (2011), <https://doi.org/10.1080/00018732.2011.624266>, URL <https://doi.org/10.1080/00018732.2011.624266>.
 - ³⁰ L. Hofstetter, A. Geresdi, M. Aagesen, J. Nygård, C. Schönenberger, and S. Csonka, Phys. Rev. Lett. **104**, 246804 (2010), URL <https://link.aps.org/doi/10.1103/PhysRevLett.104.246804>.
 - ³¹ D. Beckmann, H. B. Weber, and H. v. Löhneysen, Phys. Rev. Lett. **93**, 197003 (2004), URL <https://link.aps.org/doi/10.1103/PhysRevLett.93.197003>.
 - ³² J. Martinek, Y. Utsumi, H. Imamura, J. Barnaś, S. Maekawa, J. König, and G. Schön, Phys. Rev. Lett. **91**, 127203 (2003), URL <https://link.aps.org/doi/10.1103/PhysRevLett.91.127203>.
 - ³³ A. N. Pasupathy, R. C. Bialczak, J. Martinek, J. E. Grose, L. A. K. Donev, P. L. McEuen, and D. C. Ralph, Science **306**, 86 (2004), ISSN 0036-8075, <https://science.sciencemag.org/content/306/5693/86.full.pdf>, URL <https://science.sciencemag.org/content/306/5693/86>.
 - ³⁴ J. R. Hauptmann, J. Paaske, and P. E. Lindelof, Nature Physics **4**, 373 (2008).
 - ³⁵ M. Gaass, A. K. Hüttel, K. Kang, I. Weymann, J. von Delft, and C. Strunk, Phys. Rev. Lett. **107**, 176808 (2011), URL <https://link.aps.org/doi/10.1103/PhysRevLett.107.176808>.
 - ³⁶ B. Dong, H. L. Cui, S. Y. Liu, and X. L. Lei, Journal of Physics: Condensed Matter **15**, 8435 (2003), URL <https://doi.org/10.1088%2F0953-8984%2F15%2F49%2F019>.
 - ³⁷ I. Weymann and K. P. Wójcik, Phys. Rev. B **92**, 245307 (2015), URL <https://link.aps.org/doi/10.1103/PhysRevB.92.245307>.
 - ³⁸ D. Futterer, M. Governale, M. G. Pala, and J. König, Phys. Rev. B **79**, 054505 (2009), URL <https://link.aps.org/doi/10.1103/PhysRevB.79.054505>.
 - ³⁹ D. Futterer, M. Governale, and J. König, EPL (Europhysics Letters) **91**, 47004 (2010), URL <https://doi.org/10.1209%2F0295-5075%2F91%2F47004>.
 - ⁴⁰ I. Weymann and P. Trocha, Phys. Rev. B **89**, 115305 (2014), URL <https://link.aps.org/doi/10.1103/PhysRevB.89.115305>.
 - ⁴¹ G. Michałek, B. R. Bułka, T. Domański, and K. I. Wysokiński, Phys. Rev. B **88**, 155425 (2013), URL <https://link.aps.org/doi/10.1103/PhysRevB.88.155425>.
 - ⁴² G. Michałek, T. Domański, B. R. Bułka, and K. I. Wysokiński, Scientific Reports **5**, 14572 (2015).
 - ⁴³ G. Kotliar and A. E. Ruckenstein, Phys. Rev. Lett. **57**, 1362 (1986), URL <https://link.aps.org/doi/10.1103/PhysRevLett.57.1362>.
 - ⁴⁴ B. Dong and X. L. Lei, Phys. Rev. B **63**, 235306 (2001), URL <https://link.aps.org/doi/10.1103/PhysRevB.63.235306>.
 - ⁴⁵ B. Dong and X. L. Lei, Journal of Physics: Condensed Matter **13**, 9245 (2001), URL <https://doi.org/10.1088%2F0953-8984%2F13%2F41%2F314>.
 - ⁴⁶ B. Dong and X. L. Lei, Phys. Rev. B **65**, 241304 (2002), URL <https://link.aps.org/doi/10.1103/PhysRevB.65.241304>.
 - ⁴⁷ J. Ma, B. Dong, and X.-L. Lei, Communications in Theoretical Physics **43**, 341 (2005), URL <https://doi.org/10.1088%2F0253-6102%2F43%2F2%2F029>.
 - ⁴⁸ F. S. Bergeret, A. L. Yeyati, and A. Martín-Rodero, Phys. Rev. B **74**, 132505 (2006), URL <https://link.aps.org/doi/10.1103/PhysRevB.74.132505>.